



The Impact of Multi-Nozzles Array on Entrainment Mass Flow Rate and Homogeneity of the Speed and Profiles of Heat

Sarjito^{1*}, Denis Marchant², Yufeng Yao³, Binyamin⁴

¹Mechanical Engineering Department, Faculty of Engineering,
Universitas Muhammadiyah Surakarta, Jl. A. Yani Tromol Pos 1 Pabelan Kartasura 57102

²Faculty of Science Engineering and Computing, Kingston University,
Friars Avenue, Roehampton Vale London SW15 3DW, UK

³Faculty of Environmental and Technology, University of the West of England, United Kingdom.

⁴Department of Mechanical Engineering, Faculty of Science and Technology,
Universitas Muhammadiyah Kalimantan Timur, Jl. Ir. H. Juanda, No.15, Samarinda, Indonesia

*Corresponding author E-mail: sarjito@ums.ac.id

Abstract

The aims of the research work described in this paper are to use computational fluid dynamics (CFD) to investigate the impact of the downdraught mass flow rate generated and the homogeneity of the speed and heat profiles downstream of the multi-nozzles array. This included a work to define the optimum number, and the most effective arrangement of spray nozzles in a multi-nozzle array. Two different basic arrangements of the nozzles were studied; one in which a constant radius of 0.75 m was kept for the nozzle pitch circle as nozzles were added, and another, in which a constant distance of 0.75 m was guarded between all nozzles. A second simulation was set up using the configuration with constant spacing but with a single central nozzle embedded. A final simulation was carried out to determine if further optimization of the nozzle configuration could be obtained by altering the constant nozzle spacing in the range 0.35 to 0.85 m. Based on these simulations, it was determined that constant spacing provided greater cooling with fewer nozzles than the configurations with constant radius. Furthermore, it was found that the arrangement with 11 nozzles, with a nozzle spacing of 0.65 meters, gave the optimum overall performance.

Keywords: Computational Fluid Dynamics, Downdraught mass flow rate, Multi-array nozzle configuration, cooling power.

1. Introduction

The passive downdraught evaporative cooling system might be fully-equipped with a wetted pad mode or water spray mode using an atomizer [1], but the excess water still remaining is a problem that is not easy to manage. In a multi-nozzle array of identical nozzles at the same driving pressure, the spray water mass flow will be directly proportional to the number of nozzles used. However, the number of nozzles and their relative positions will affect thermal energy and momentum transfer due to the increasing interference between the individual spray cones when additional nozzles are added. It was expected that eventually, the inclusion of additional nozzles would offer no advantage, and that an optimum configuration could be identified.

A possible alternative approach which might offer some advantages would be to add additional nozzles while keeping the total spray water mass flow constant. While this approach would be theoretically possible, the subdivision of the constant total spray water flow each time an additional nozzle was added, would require the use of different nozzles of progressively smaller orifice diameter at each stage, and might also require a change in the driving pressure. Additionally, the droplet size distribution generated by the nozzles would change at each stage. This alternative approach was not considered further and the investigations described in this paper used the same mass flow rate at each stage.

For the purpose of verification of the software, modelling and testing of a CFD model using a single spray nozzle in a vertical cylinder has been carried out [2]. The model, which simulated both the water mist evaporation process and the thermal energy and momentum transfer between the droplets and the surrounding air, was developed with the objective of validating the basic spray modelling methodology used in the present work by reproducing the results for a single spray nozzle model produced by Gant at the UK Health and Safety Laboratory, (HSL), Buxton [4]. The result of the simulation was compared with the experimental data of a single spray model carried out by St. George and Bucklin [5], resulting in good agreement, although the velocity at the centre downstream to the nozzles was slightly lower. Further development work on the model to incorporate two commercially available nozzles, (BETE PJ32 and TF6) [6], and calculations to ensure that the results were theoretically and physically sensible are also described [2]. Results from recent experiments [7], which were carried out specifically to check the validity of the droplet evaporation model in the Ansys CFX software were also a motivation for this work. However, refer to some references the above, on that implementation, there has not been state clearly, whether or not accountable optimization has been done, and it was still question mark, particularly number of nozzles used and its nozzle configu-

ration. Therefore, in this work the investigation will be focused in determining optimum number of nozzles and possibility of its nozzle position, in order to have better entrainment mass flow and homogeneity of temperature distribution at downstream of the cooling tower.

2. Modelling of multi-nozzle array of identical nozzles

The flow domain for these studies was created as a vertical cylinder with overall length and diameter at $D = 4$ m and $L_0 = 3$ m respectively.

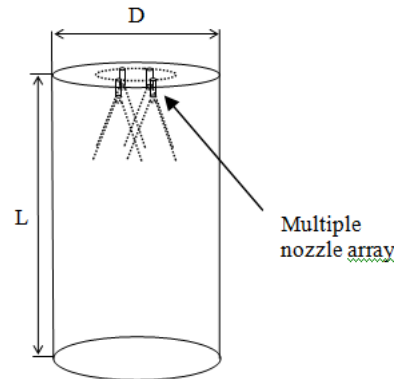


Fig. 1: Flow Domain dimensions for multiple nozzle simulations

The evaporation modelling and droplet size distribution were set up with a single downward-facing nozzle at the centre of the upper circular face. The nozzle was modelled as a cylinder of diameter $d_0 = 0.00625$ m and length 0.05 m, as shown on top in Figure 1. Within CFX [7] in the present work, a droplet diameter distribution was specified as a series of mass and number fractions in discrete diameter bands. This approach was adopted corresponding to the TF6 nozzles used with a water droplet mass flow rate of 0.096 kg/s and a spray velocity of 21.57 m/s, for a water temperature of 10°C, and a CFX input data set using 1500 particles to represent the droplet population, and was created from information based on mass and number fraction data sets summed to unity exactly, that at least one representative particle was present in each diameter band, and data was given in references [9] at a driving pressure of 3.33 bar:

Droplet diameter bands (μm)

27, 55, 82, 106, 121, 136, 152, 171, 193, 230, 256, 282, 307, 339, 381, 425

Mass fraction per band

0.0029,0.0100,0.0217,0.0387,0.0550,0.0745,0.0963,0.1136,0.1195,0.1119,0.0959,0.0800,0.0652,0.0502,0.0371,0.0273

Number fraction per band

0.3438,0.1379,0.0915,0.0758,0.0727,0.0686,0.0641,0.0529,0.0389,0.0214,0.0133,0.0083,0.0053,0.0030,0.0016,0.0008

In setting up the flow physics a reference temperature of 25°C, a reference pressure of 1 atmosphere, and a reference air density of 1.2 kg/m³ were used. The boundary condition on both the upper and the lower circular faces of the flow domain was set as an opening, which permitted both inflow and outflow from the flow domain, and a free-slip adiabatic wall condition was specified at the cylinder surface. Buoyancy effects were modelled using the standard density difference model within CFX combined with an acceleration of -9.81 m/s² in the Y direction.

Within the flow domain, a variable composition gas mixture of air and water vapour was set up, with the water droplet being set up as a dispersed liquid phase. Drag forces on the liquid droplet were modelled by the Schiller Naumann equation. This drag model is based on the assumptions that the fluid droplets within the spray were sufficiently small to be considered spherical and that the volume fraction of the droplets was small. These assumptions were considered to be reasonable. Interphase thermal energy transfer was modelled using the Ranz Marshall (Nusselt number based) correlation, (ANSYS CFX 13-Solver theory guide 2010) [8]. Droplet evaporation was modelled using the standard evaporation model within CFX, in which the saturated vapour pressure is correlated as a function of temperature through the Antoine equation:

$$p_{sat} = \exp\left(A - \frac{B}{T + C}\right) \quad (\text{bar}) \quad (1)$$

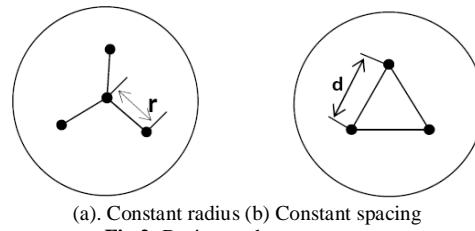
where T is the temperature in kelvin and the constants A , B and C are 5.11564ln(10), 1687.54ln(10) and -42.92 respectively.

For turbulence modelling, both the shear stress transport (SST) and k-epsilon models were used with automatic wall functions. In both cases, the inlet turbulence intensity level was set to 5%.

At the spray inlet, the droplet injection region was specified using the standard cone injection method within CFX. Since the Lagrangian model does not accurately simulate primary droplet break-up, the injection centre was placed 0.01 m below the nozzle outlet plane. The cone angle was ϕ specified as 90° with full cone injection. Using a larger number of droplets gave a smoother distribution of results, but also increased the computing time and memory needed.

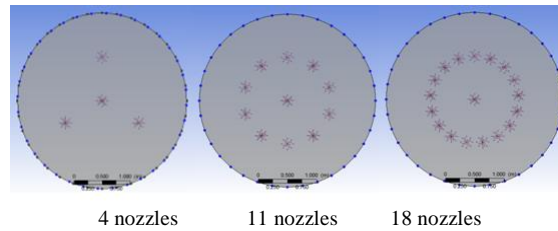
3. Investigation of multiple nozzle configurations

Two basic arrangements of the nozzles were investigated; a configuration, (Figure 2(a)), in which a constant radius, $r = 0.75$ m was maintained for the nozzle pitch circle as nozzles were added, and a configuration, (Figure 2(b)), in which a constant separation distance $d = 0.75$ m was maintained between all nozzles.

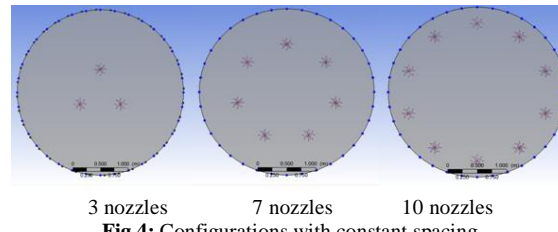


(a). Constant radius (b) Constant spacing
Fig 2: Basic nozzle arrangements

A range of constant radius configurations using from 3 to 20 nozzles was simulated. The configurations with 4, 11 and 18 nozzles are shown in Figure 3.



4 nozzles 11 nozzles 18 nozzles
Fig 3: Constant radius configurations



3 nozzles 7 nozzles 10 nozzles
Fig 4: Configurations with constant spacing

A range of configurations with constant spacing using from 3 to 12 nozzles was also simulated. The configurations with 3, 7 and 10 nozzles are shown in Figure 4.

The surface and volume meshes were created using minimum and maximum face spacings of 0.002 m and 0.02 m, with an angular resolution of 30°, and a body spacing of 0.02 m. These settings produced approximately 1,455,000 tetrahedral elements for the simulations using 3 nozzles, and 3,655,000 tetrahedral elements for the simulation using 20 nozzles. The inlet boundary condition at the upper circular face was specified as an opening with an incoming air temperature of 30°C and 0% relative humidity. The boundary condition at the lower circular face was specified as an outlet at atmospheric pressure. A free-slip adiabatic wall condition was set on the cylinder surface. Steady-state simulations were carried out using a physical time scale control 0.05s with a residual target of 1e-6 and using the k-epsilon turbulence model with the inlet turbulence level set to 5%.

The variations in average outlet temperature and in total mass flow rate for all configurations are shown in Figure 5

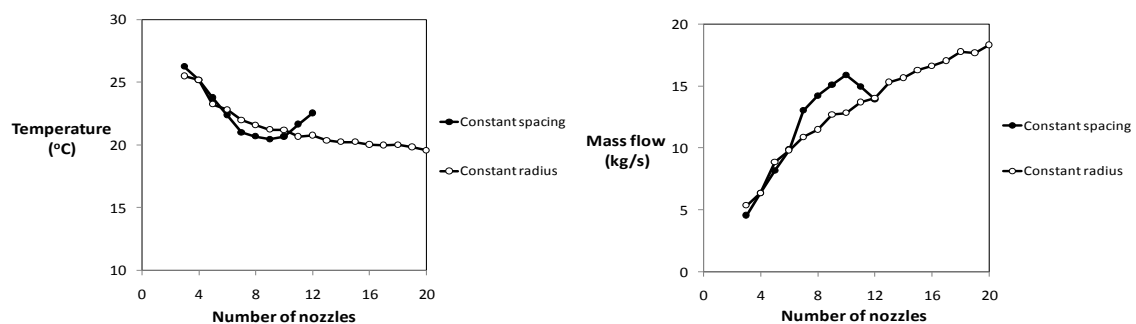


Fig 5: Variation in outlet temperature and mass flow with nozzle configuration

It can be seen from Figure 5 that the constant radius configuration produced the lowest overall temperature and the highest mass flow rate, but used more nozzles to produce these effects than the configuration with constant spacing. In particular, for numbers of nozzles between 6 and 11 the configuration with constant spacing was more effective at both reducing the average outlet temperature and entraining the air flow. The best cooling performance was obtained with 9 nozzles and the highest entrainment rate with 10 nozzles.

Based on these results a second series of simulations was set up using the configuration with constant spacing to investigate the effect of adding a central nozzle to the 8 to 12 nozzle configurations.

4. Constant spacing configuration with central nozzle

A second series of simulations was set up using the configuration with constant spacing, with a single central nozzle added. The configurations investigated used 8 to 12 nozzles. In all cases a constant nozzle spacing of $d = 0.75$ m was maintained. Contour plots showing the outlet temperature distributions range of 283.1 - 303.1 K obtained are shown in Figure 6.

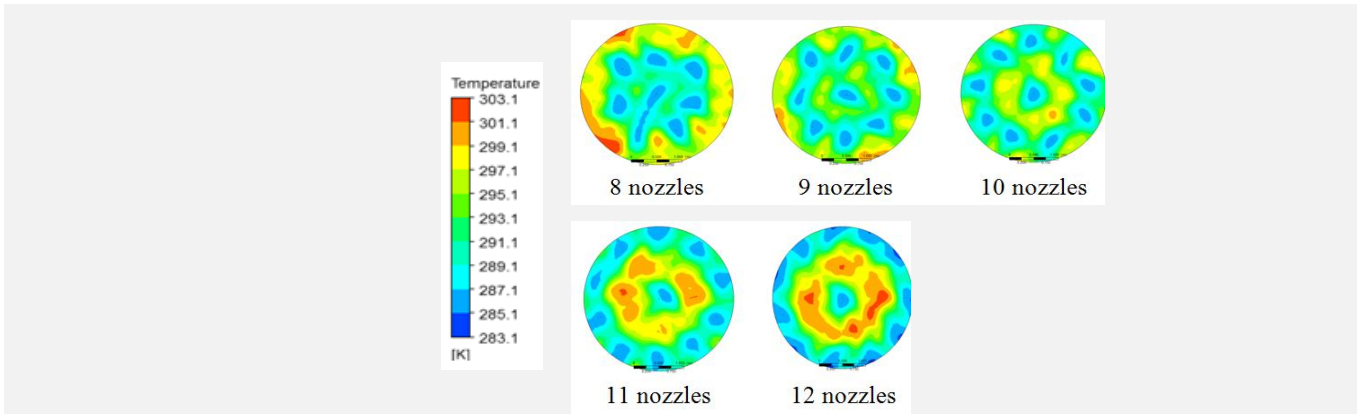


Fig 6: Outlet temperature distributions, configurations with constant spacing and a single central nozzle

By comparing the image for the case with 11 nozzles in Figure 6 with the result for the case with 10 nozzles without a central nozzle, a significant improvement in cooling in the central region was observed. Figure 7 shows a contour plot of the outlet temperature distributions for configurations with constant spacing without a central nozzle and with a single central nozzle.

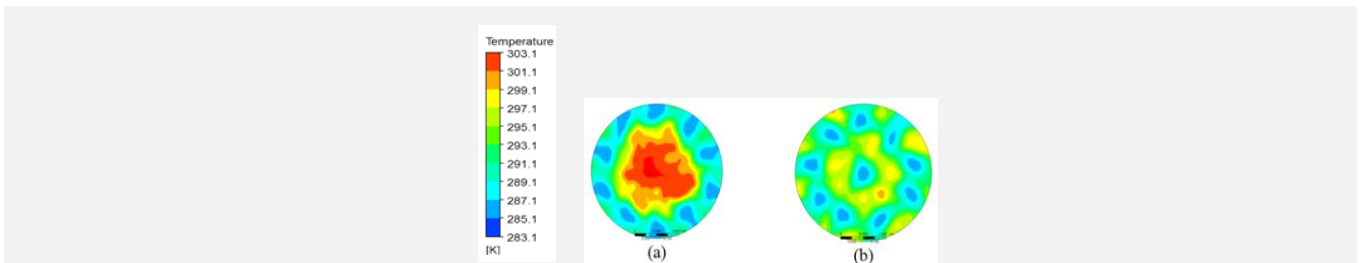


Fig 7: Outlet temperature distributions for configurations with constant spacing without a central nozzle (a) and with a single central nozzle (b)

The variations in average outlet temperature and in total mass flow rate obtained for all configurations are shown in Figure 8 together with the previous results shown in Figure 5 for comparison.

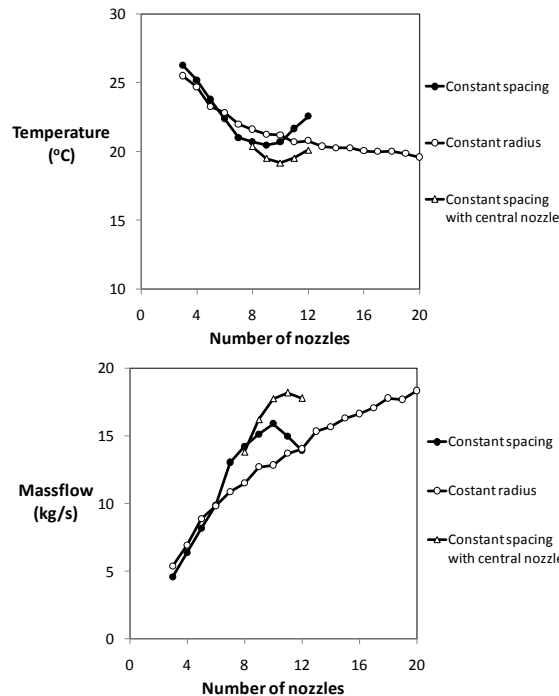


Fig 8: Variation in average outlet temperature and mass flow, (showing additional configurations with constant spacing and single central nozzle)

It can be seen from Figure 8 that the configurations with the additional central nozzle produced both lower average outlet temperatures and higher entrained mass flow rate in all cases. The best cooling performance was obtained with 10 nozzles and the highest entrainment rate with 11 nozzles.

Based on these results a third series of simulations was carried out to investigate if further optimization of the nozzle configuration could be achieved by altering the constant nozzle spacing. The configuration selected for these further studies was the 11-nozzle configuration. This configuration was selected because it produced the highest entrainment rate.

5. Optimization of nozzle separation

These simulations were carried out for constant nozzle spacings d ranging from 0.35 to 0.85 m in 0.1 m steps. The simulations were carried out using an incoming air temperature of 30°C and 0% relative humidity and spray water temperature of 10°C. The variations in average outlet temperature and mass flow rate with nozzle spacing are shown in Figure 9.

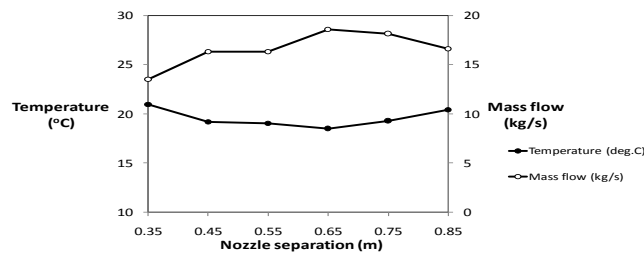


Fig 9: Variation in average outlet temperature and mass flow with nozzle spacing for 11-nozzle configuration with central nozzle

It can be seen from Figure 9 that the configuration with the 0.65 metre nozzle spacing produced both the lowest average outlet temperature and the highest entrained mass flow rate. Based on these results this nozzle spacing of 0.65 was selected for use in all future studies.

6. Cooling power for optimum nozzle configuration

For evaporative cooling the sensible cooling power can be estimated from the induced mass flow rate and temperature reduction of the air flow. This calculation was carried out for the optimum arrangement of 11 nozzles and the result is discussed in a separate study. Theoretically, the optimum cooling power could be achieved by utilising finer droplets and providing sufficient rest time to evaporate the droplets. A separate specific study, which is not considered within this paper, was carried out to investigate the correlation between the cooling power and the length of the cylinder; however, no study has been performed to investigate the correlation between cylinder length and diameter with droplet size.

7. Conclusions

CFD simulations were carried out to define the optimum number, and the most effective arrangement of spray nozzles in a multi-nozzle array. Two basic arrangements of the nozzles were investigated; one in which a constant radius of 0.75 m was maintained for the nozzle pitch circle as nozzles were added, and another, in which a constant separation distance or spacing of 0.75 m was maintained between all nozzles. Based on these simulations it was concluded that configurations with constant spacing, utilising 6 – 11 nozzles, provided greater cooling than the configurations with constant radius and using more nozzles.

A second series of simulations was set up using the configuration with constant spacing, with a single central nozzle added. It was concluded that this arrangement produced both lower average outlet temperatures and higher entrained mass flow rates in all cases and that the arrangement with 11 nozzles gave the best overall performance.

A further series of simulations were carried out to determine if further optimization of the nozzle configuration could be obtained by altering the constant nozzle spacing in the range 0.35 to 0.85 m. It was concluded that a further improvement in performance could be achieved by setting the nozzle spacing to 0.65 m and this configuration would be selected for use in all future studies.

A future work recommendation may be done by configuring nozzles position for some nozzle at the upper level and some nozzles at the lower position or probably in helical configurations.

Acknowledgement

My first thanks must go to Dr George Simpson formally at Kingston University London, for helpful discussion in preparing the work. Also, Authors would like to thank to Universitas Muhammadiyah Surakarta (UMS) for providing research funding and supporting international publications.

References

- [1] Pearlmutter, D., Erell, Y. (2008), "A novel multi-stage down-draft evaporative cool tower for space cooling. Part 2: Preliminary experiments with a water spraying system," *Solar Energy*, (82), pp. 430–440.
- [2] Sarjito (2012), "An investigation of the design and performance of a multi-stage downdraught evaporative cooler", Unpublished thesis, Kingston University, London, UK (1996) 53-88.
- [3] Sarjito and Marchant D (2013), Effect of downdraught mass flow rate generated and the uniformity of the velocity and temperature profiles downstream of the multi-array nozzles, 13th International Conference Proceeding on Quality in Research (QIR), Yogyakarta, Indonesia, eprints.kingston.ac.uk
- [4] Gant, S. E. (2006) 'CFD Modelling of Water Spray Barriers', HSL (79), Harpur Hill, Buxton Derbyshire, SK17 9JN. UK.
- [5] St. George, M. and Buchlin, J. M. (1994) 'Detailed single spray experimental measurements and one-dimensional modelling', *Int. J. Multiphase flow*, (20), pp.979-992.
- [6] BETE TF6 nozzles, data sheet (2007), available information on <http://www.beteuk.com>
- [7] Lim, E.W.C., Koh, S.H., Lim, L.K.b, Ore, S.H, Tay, B.K, Ma, Y., and Wang, C.H., (2008) 'Experimental and computational studies of liquid aerosol evaporation', *Aerosol Science*, (39), pp. 618 – 634.
- [8] ANSYS 12.1 and 13.0 CFX-Solver Manager User's Guide, (2010).
- [9] Tambur, Y. and Gueta, S., "Optimizing the design and operation of the sprays in the tower", Unpublished report, Faculty of Aerospace engineering, Technion-Israel Institute of Technology, Appendix B., Israel. (2006), (Private communication by email).